Fragmentation of long-lived hydrocarbons after strong field ionization

Seyedreza Larimian,[1] Sonia Erattupuzha,[1] Erik Lötstedt,[2,*] Tamás Szidarovszky,[2] Raffael Maurer,[1] Stefan Roither,[1] Markus Schöffler,[1] Daniil Kartashov,[1] Andrius Baltuška,[1] Kaoru Yamanouchi,[2] Markus Kitzler,[1,†] and Xinhua Xie (谢新华)[1,‡]

[1]*Photonics Institute, Vienna University of Technology, A-1040 Vienna, Austria*

[2]*Department of Chemistry, School of Science, The University of Tokyo, 7-3-1 Hongo, Bunkyo-ku, Tokyo 113-0033, Japan*

(Received 23 December 2015; published 5 May 2016)

We experimentally and theoretically investigated the deprotonation process on nanosecond to microsecond timescales in ethylene and acetylene molecules following their double ionization by a strong femtosecond laser field. In our experiments we utilized coincidence detection with the reaction microscope technique. We found that both the lifetime of the long-lived ethylene dication leading to the delayed deprotonation and the relative channel strength of the delayed deprotonation compared to the prompt one have no evident dependence on the laser pulse duration and the laser peak intensity. Quantum chemical simulations suggest that the observed delayed fragmentation process originates from the tunneling from near-dissociation-threshold C–H stretch vibrational states on a dicationic electronic state. These vibrational states can be populated through strong field double-ionization-induced vibrational excitation on an electronically excited state in the case of ethylene, and through a spin-flip transition from electronically excited singlet states to the triplet ground state in the case of acetylene.

DOI: 10.1103/PhysRevA.93.053405

I. INTRODUCTION

The timescale on which a chemical reaction takes place depends on the properties of the atoms or molecules involved and the external reaction conditions. In the past decades, femto-chemistry, based on the use of femtosecond laser pulses, has become a vivid research direction in probing and controlling chemical reactions [1,2]. Traditionally, femto-chemistry employs temporally shaped femtosecond laser pulses for steering the nuclear vibrational dynamics to control the formation or breakage of molecular bonds [3]. In recent years, laser pulses with high intensity and ultrashort duration were successfully applied to control molecular fragmentation and isomerization reactions through strong field ionization or excitation [4–10]. These molecular fragmentation processes involve one or more bond breakages during or after the interaction of a molecule with a strong laser field [11]. When exposed to a strong laser field, a molecule can be multiply ionized through multiphoton, tunneling, or over-barrier ionization, resulting in a certain charge state that may be dissociative and lead to the fragmentation of the molecular ion into several pieces. The laser-induced molecular fragmentation from a dissociative state is in most cases a fast process happening on femtosecond or picosecond timescales [12–16]. It has been reported that molecular fragmentation processes can be controlled by a strong laser field by enhancing or suppressing the population of corresponding electronic states [5,9,10]. Of particular importance is the contribution of electrons in low-lying molecular orbitals in the ionization process. Removing electrons from low-lying molecular orbitals may put the molecular ion into a dissociative electronically excited state [5,10,17]. The dissociative state usually decays quickly after strong field ionization. However, due to the complex potential-energy structure of molecular dissociative states, they can cross with other electronic states, which can open up several possible fragmentation pathways [18].

A technique that is well suited for studying strong-field-induced molecular fragmentation is reaction microscopy [19,20]. By using this technique a large number of works have studied molecular fragmentation; see, e.g., Refs. [4–10]. In all of them, the fragmentations were found to happen on a much faster timescale than the nanosecond temporal resolution of the detector and data acquisition system [11]. Here we report the observation of delayed fragmentation from hydrocarbon dications after ionization in a strong femtosecond nonresonant laser field. We observe dications with lifetimes ranging from hundreds of nanoseconds to microseconds. Our results suggest that this delayed fragmentation originates from high-lying vibrational states near the dissociation threshold. We present quantum chemical simulations which indicate that these high-lying vibrational states may be populated by vibrational excitation during strong field double ionization to an electronically excited state, or by intersystem crossing (transition between states of different spin multiplicity driven by spin-orbit coupling) [21] from an electronically excited state to the electronic ground state.

II. EXPERIMENTS

In the experiments we employ a reaction microscope to measure the three-dimensional momentum vectors of ions resulting from the laser-molecule interaction [19,20]. We use few-cycle laser pulses with a pulse duration down to 4.5 fs [full width at half maximum (FWHM) of the peak intensity], which are generated by spectral broadening and recompression of 25 fs pulses from a Ti:sapphire laser amplifier system. These pulses are guided into an ultrahigh vacuum reaction chamber ($\sim 1.3 \times 10^{-10}$ mbar) and focused onto a cold supersonic jet of molecules (diameter of ~ 170 μm). The molecular jet is prepared by supersonic expansion of the gas from a nozzle with a diameter of 10 μm and collimated by a two-stage skimmer before being sent to the reaction chamber. We carried out measurements on acetylene and ethylene. Ions produced

*lotstedt@chem.s.u-tokyo.ac.jp
†markus.kitzler@tuwien.ac.at
‡xinhua.xie@tuwien.ac.at

from the strong-field interaction with the gas beam are guided to a time- and position-sensitive detector by a homogeneous electric field (23.1 V/cm). The laser pulse duration is adjusted by introducing positive chirp by adding a certain amount of fused silica to the beam path of the shortest pulse. The laser peak intensity is varied by reflection off a glass block under different grazing incidence angles. Calibration of the peak intensity on the target was done with an estimated precision of 10% by separate measurements using single ionization of argon atoms in circularly polarized light [22]. The duration and intensity stability of the pulses were monitored on a shot-to-shot basis by a stereo-above-threshold-ionization phase meter [23,24]. More details on the experimental setup can be found in our previous publications [9,25,26].

III. RESULTS

A. Identification of delayed-fragmentation channel

First, we focus on the experiments on ethylene molecules. In previous experiments [9] we found that there are mainly three two-body fragmentation channels from ethylene dications after the strong field double ionization: deprotonation ($C_2H_3^+ + H^+$), H_2^+ formation ($C_2H_2^+ + H_2^+$), and symmetric breakup ($CH_2^+ + CH_2^+$). All three reactions proceed during or shortly after the laser interaction such that the fragmentation process takes place within the laser interaction region on a timescale much shorter than the temporal resolution of the detector and data acquisition system, which is about one nanosecond. A typical measured photoion-photoion-coincidence (PIPICO) distribution of ethylene is presented in Fig. 1(a). The PIPICO distribution reflects the correlation between the time of flights (TOFs) of two detected particles on the detector. Because of momentum conservation, the two-body fragmentation channels from ethylene dications appear as parabolic lines, which are marked in Fig. 1(a). We notice that the deprotonation channel has a weak but rather long tail while the PIPICO lines for the other two channels are short. Such long tails have been previously observed and studied in the dissociative double ionization of molecules with extreme-ultraviolet pulses [27–32]. A long PIPICO line may indicate high kinetic energy release (KER) during the two-body fragmentation. However, a long line corresponding to a high KER extends in both directions, which is not the case in Fig. 1. In addition, we simulated the PIPICO line for a deprotonation process with a high KER and found that the measured long PIPICO line does not follow the simulated one. Therefore, we conclude that the long tail does not come from a fragmentation process leading to a high KER.

A long PIPICO line can also be formed by fragmentation happening long after the laser-induced double ionization, during the flight of the dications to the detector. To investigate whether the long PIPICO line is caused by such a fragmentation process, we simulated the TOFs of $C_2H_3^+$ and H^+ for the case in which there is a time delay between ionization and fragmentation. Before fragmentation, the ethylene dication flies towards the detector due to the weak dc field applied in the spectrometer. At the time of fragmentation, the dication breaks into a proton and $C_2H_3^+$ which then both separately fly towards the detector and hit it at different times and positions according

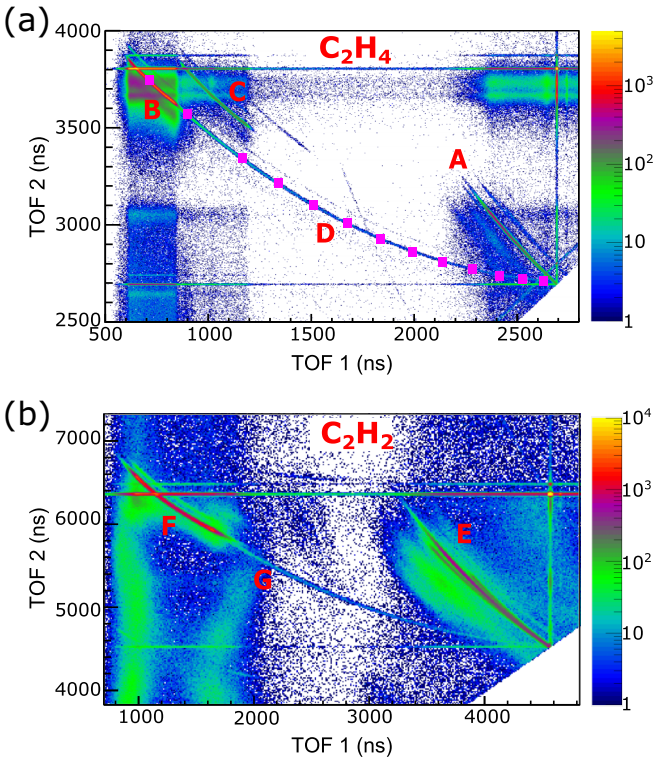

FIG. 1. Photoion-photoion-coincidence (PIPICO) distributions of (a) ethylene (with a dc field strength of 23.1 V/cm) and (b) acetylene (with a dc field strength of 7.5 V/cm) in a linearly polarized strong laser field with a peak laser intensity of 3×10^{14} W/cm^2 and a pulse duration of 4.5 fs. A: $CH_2^+ + CH_2^+$; B: $C_2H_3^+ + H^+$ (prompt); C: $C_2H_2^+ + H_2^+$; D: $C_2H_3^+ + H^+$ (delayed); E: $CH^+ + CH^+$ and $C^+ + CH_2^+$; F: $C_2H^+ + H^+$ (prompt); G: $C_2H^+ + H^+$ (delayed). The magenta squares indicate simulated PIPICO points for the delayed deprotonation process with a certain time delay between the ionization and the fragmentation process.

to their mass and charge. We solve Newton's equations for the motion of these charged particles in a dc field to obtain their TOFs:

$$\tfrac{1}{2}a_i(\mathcal{T}_i - T)^2 + v_i(\mathcal{T}_i - T) + z = L, \qquad (1)$$

where $\mathcal{T}$ is the time of flight, index $i = 1,2$ refers to two different moieties after the fragmentation, a is the acceleration of the particle in the spectrometer direction by the applied dc electric field, T is the delay between the ionization and fragmentation (survival time of the dication), v is the velocity of the particles at the time of fragmentation along the spectrometer, which can be found from initial conditions and the conservation of momentum at the time of fragmentation, $z = \frac{1}{2}a_0T^2$ is the position of the intact dication within the spectrometer along the dc field direction at the time of fragmentation (a_0 is the acceleration of the dication by the applied dc electric field) and L is the distance between the interaction point and the ion detector. The initial momentum of the parent ion is assumed to be zero. We vary the time delay T and overlay the simulated TOFs of the two ions onto the measured data shown as magenta points in Fig. 1(a). These points perfectly overlap with the measured long PIPICO line. This proves that the long PIPICO line originates from a deprotonation

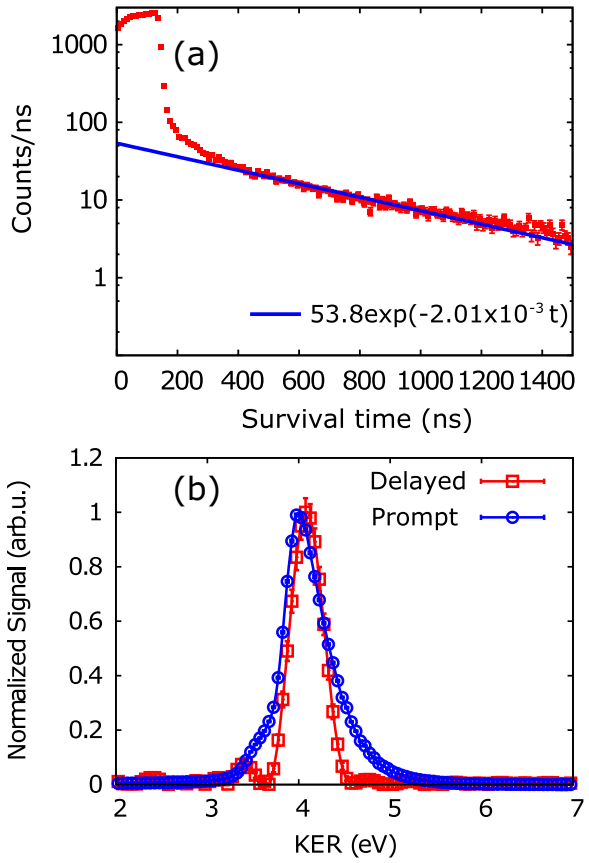

FIG. 2. (a) Retrieved survival time distribution of the ethylene dication before the delayed deprotonation process with an exponential fit of $53.8\exp(-2.01\times10^{-3}t)$. (b) KER distributions of the prompt (blue circles) and the delayed (red squares) deprotonation processes. The energy resolution is about 0.4 eV at KER $\approx$ 4 eV.

process with a long survival time of the ethylene dication after double ionization. In the measurements on acetylene, the PIPICO distribution of which is presented in Fig. 1(b), we observed a similar deprotonation process. Additionally, the delayed deprotonation is observed also in measurements of ethylene and acetylene fragmentation induced by circularly polarized laser pulses.

B. Lifetimes and kinetic-energy-release distributions

From the measured data we select the long PIPICO line by applying the known relation between the TOFs of the two ions fulfilling momentum conservation derived from Newton's equations and their impact positions (x,y) on the detector to ensure coincidence selection. This minimizes the contributions from background signals. We retrieve the survival time of the ethylene dications by using the relation derived from Newton's equations for the ion pair fulfilling momentum conservation:

$$T = \frac{(a_0-a_2)(a_1\mathcal{T}_1^2-2L)-(a_0-a_1)(a_2\mathcal{T}_2^2-2L)}{2(a_0-a_2)(a_0-a_1)(\mathcal{T}_2-\mathcal{T}_1)}. \quad (2)$$

The distribution of the survival time for the ethylene dication is shown in Fig. 2(a). Note that the peak of the survival time distribution below 200 ns originates from the prompt fragmentation. This peak forms due to the application of Eq. (2) to the region where hits from the prompt and delayed processes overlap. The retrieved survival-time distribution presented in Fig. 2(a) is meaningful only for the delayed process. Therefore, in the following we only consider the data points with a survival time longer than 400 ns, which exclusively originate from the long-lived dications. The figure clearly shows that yield of the ethylene dications undergoing delayed deprotonation decays exponentially. We fit the measured signal with an exponential function $S(t) = S_0e^{-\alpha t}$, shown as the blue solid line in Fig. 2(a), which yields the decay rate $\alpha = (2.01 \pm 0.05) \times 10^{-3}$ ns^{-1}. From the fit parameter α, we obtain the lifetime of ethylene dications for the delayed deprotonation channel as $1/\alpha = 498 \pm 12$ ns.

For a certain TOF the retrieved momentum distribution of the delayed deprotonation process in the detector plane is a projection of the three-dimensional (3D) momentum sphere onto a two-dimensional (2D) plane. Therefore, to obtain the correct 3D momentum distribution, an Abel transform needs to be applied to the raw momentum distribution [33]. From the retrieved momentum we can then obtain the KER of the delayed deprotonation process shown in Fig. 2(b). The mean value of the KER distribution is 4.1 eV (with a FWHM of 0.4 eV), which is almost the same as that of the prompt deprotonation process, for comparison also shown in Fig. 2(b). Additionally, by selecting different survival-time intervals we find that the KER distribution does not depend on the survival time of the ethylene dication. This indicates that all delayed deprotonation events may originate from the same initial state.

C. Dependence of lifetime and channel strength on laser parameters

In previous studies we found that strong field induced molecular fragmentation processes strongly depend on the parameters of the laser pulse, such as duration, peak intensity, and carrier-envelope phase [5,9,34–36]. As shown in Ref. [9], the relative channel strength between the deprotonation process and the stable ethylene dication has a strong dependence on the laser pulse duration. To investigate the origin of the deprotonation process from the long-lived dications observed here, especially its relation to the prompt deprotonation process, we performed measurements on ethylene with different pulse durations from 4.5 fs up to 25 fs and peak intensities ranging from 5×10^{14} W/cm^2 to 8×10^{14} W/cm^2. The pulse duration was adjusted between 4.5 and 17 fs by positively chirping the shortest pulses by propagating them through different lengths of fused silica. Pulses with a duration of 25 fs are used directly from the laser amplifier. In the data analysis we obtain the decay rate of the ethylene dication for the delayed deprotonation from the exponential fitting. Because of the overlapping with the strong prompt deprotonation signal, shown in Fig. 2(a), it is impossible to directly obtain the yield of the deprotonation channel from the long-lived dications. However, we can obtain the yield indirectly by integrating the exponential fitting function over the survival time, which leads to $N_0 = \int_0^\infty S_0e^{-\alpha t}\,dt = S_0/\alpha$, with S_0 and α being the fitting coefficients. For the prompt deprotonation channel with a time delay between ionization and fragmentation shorter than 1 ns, we performed the usual coincidence momentum

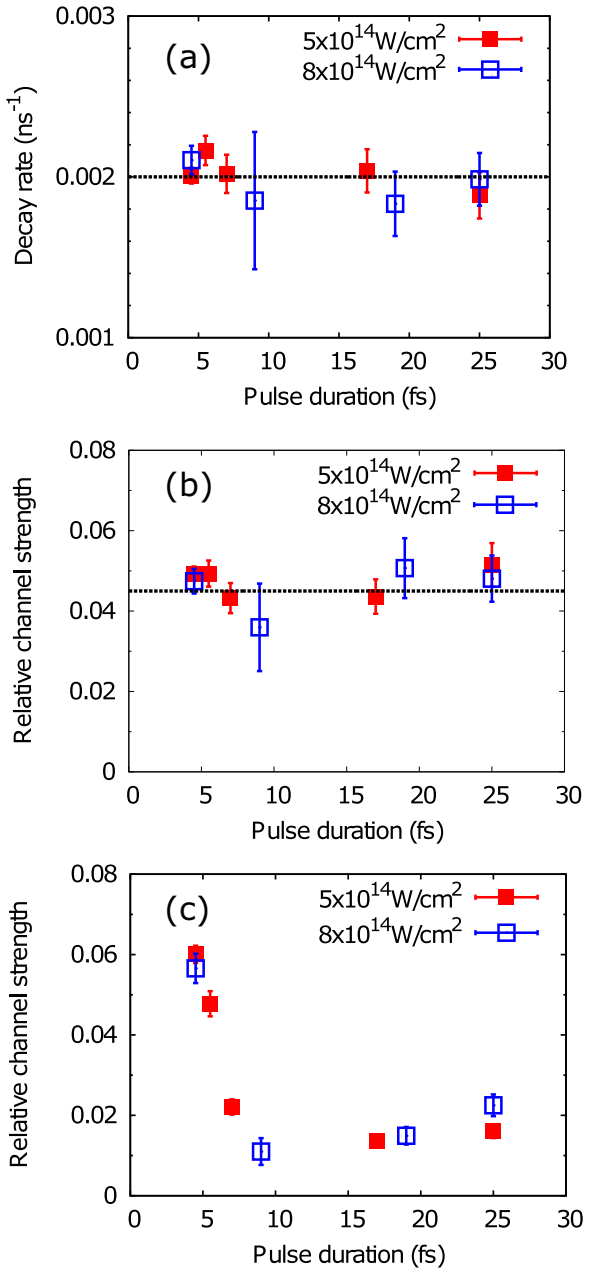

FIG. 3. (a) Retrieved decay rate of ethylene dications for the delayed deprotonation process as a function of laser pulse duration for laser peak intensities of 5×10^{14} W/cm^2 and 8×10^{14} W/cm^2. (b), (c) Retrieved relative channel strength of the delayed deprotonation process with respect to the prompt one (b) and the detected dication (c). The horizontal lines in panels (a) and (b) indicate the average values of the measurements.

retrieval and applied momentum conservation conditions in all three dimensions [9]. The such obtained relative channel strength of the delayed deprotonation to the prompt one is about 4.5%. The decay rate and the relative channel strength as a function of laser pulse duration are presented in Figs. 3(a) and 3(b), respectively, for two laser intensities. It can be seen that both the decay rate and the relative strength of these two processes have no evident dependence on the laser pulse duration and intensity. No dependence of the decay rate on the laser parameters indicates that all delayed deprotonation events originate from the decay of the same vibronic states of the ethylene dication. In addition, no laser parameter dependence of the relative channel strength denotes that both processes originate from the same nuclear wave packet on the same potential-energy surface, which is populated after the strong field double ionization. No dependence on the laser parameters also indicates that the vibronic states with a long lifetime, leading to the delayed deprotonation, are not populated by laser-induced excitation from lower-lying states. Note, however, that the strength of the delayed deprotonation signal relative to the dication signal, plotted in Fig. 3(c), shows a significant dependence on the laser pulse duration. This indicates that the delayed deprotonation originates from a different state than the stable dication, which is observed when the electronic ground state is populated [9].

IV. DISCUSSION

In the following we discuss the mechanism behind the long lifetime of ethylene dications that leads to the delayed deprotonation process.

In recent studies we found that electronically excited states of the ethylene dication are dissociative and lead to various fragmentation processes, such as deprotonation, symmetric breakage, or H_2^+ formation [5,9]. The electronic ground state of the ethylene dication is metastable and has a very long lifetime, which might be a candidate for the mentioned deprotonation process [9]. However, based on the same dependence on laser pulse duration and intensity of the delayed and prompt deprotonation processes, we conclude that both processes may originate from the same electronic state. In Ref. [9] it was shown that the prompt deprotonation originates from electronically excited states populated by removal of at least one HOMO-1 electron, while the other excited states, which involve removal of electrons from HOMO-2, preferentially lead to C–C breakage. Therefore, an involvement of the electronic ground state can be ruled out. On the other hand, for the electronically excited states that lead to C–C breakage, there exists no energy barrier along the C–C stretching coordinate, which explains why we do not observe a delayed C–C breakage process in our measurements.

To obtain insight into the electronically excited states which might lead to the long-lived dications we computed the PECs of the ethylene dication with the planar geometry (the equilibrium geometry of neutral ethylene) along a C–H stretching coordinate. Here the complete active space self-consistent field method [6-311++G(d,p) basis set] as implemented in GAMESS [37] was used, with 10 active electrons in 12 orbitals. A one-dimensional potential energy curve (PEC) was obtained by varying one of the C–H bond lengths in $C_2H_4^{2+}$, while all other bond lengths and bond angles were kept fixed at the values corresponding to the equilibrium structure of neutral C_2H_4. The PECs of the electronic ground state $^1A'$, the lowest electronically excited triplet state $^3A''$ (formed by removing one HOMO and one HOMO-1 electron with the same spin) and the lowest electronically exited singlet state $^1A''$ (formed by removing one HOMO and one HOMO-1 electron with opposite spin) are presented in Fig. 4(a) as the gray, blue, and green lines, respectively. The PECs of the two excited

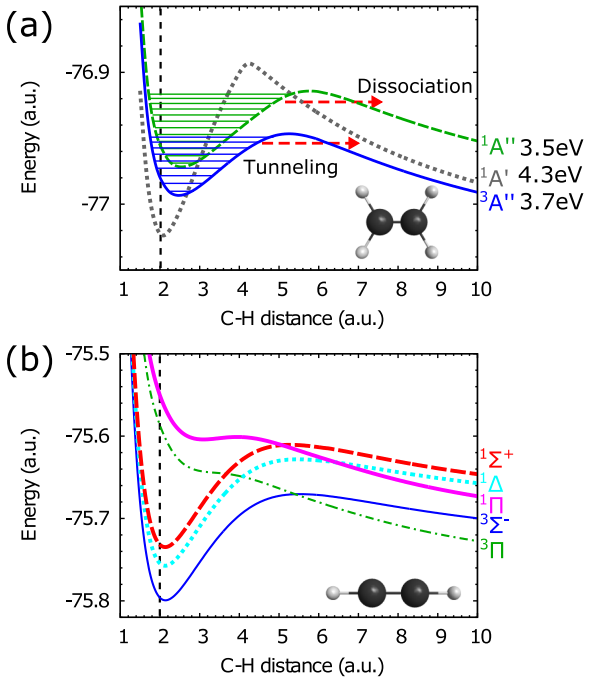

FIG. 4. (a) Calculated PECs along a C–H stretching coordinate of the planar ethylene dication. The gray dotted line corresponds to the electronic ground state, while the blue solid line and the green dashed line present the first and second electronically excited states, respectively. The horizontal lines represent the vibrational levels. The numbers beside the state symbols are estimated KERs of the dissociation limit from each state. (b) Calculated PECs along a C–H stretching coordinate of the acetylene dication, with all other coordinates fixed in the neutral equilibrium geometry. The vertical dashed lines are the equilibrium C–H distances of the neutral molecules.

states show barriers along the C–H stretching coordinate with a height of about 1.5 and 1.2 eV, respectively, which might support a long lifetime of the dication prior to deprotonation. When a nuclear wave packet is created in a vibrational level close to the dissociation threshold, it can tunnel through the potential barrier resulting in delayed deprotonation.

Utilizing the complex coordinate scaling method [38] we calculated the quasibound vibrational energies (relative to the minimum of the potential well) and lifetimes [39] supported by the one-dimensional PECs for the first excited (triplet) state $^3A''$ and the second excited (singlet) state $^1A''$ in $C_2H_4^{2+}$, as listed in Tables I and II.

We obtain lifetimes of 2.53 ns and 1.3 μs for the second ($\nu = 8$) and the third ($\nu = 10$) highest vibrational levels of the first and the second electronically excited states, respectively, which are on the same timescale of the experimentally obtained value of 498 ns. The theoretical calculations thus support the hypothesis of near-dissociation-threshold tunneling as the origin of the long-lived dications. By slightly varying the PECs, we confirmed that the lifetimes of the high-lying vibrational states are very sensitive to the exact shape of the potential. A slight change of the barrier height can result in an order-of-magnitude change of the lifetime. Additionally, lifetimes can also be sensitive to rotational excitation; therefore, it is not meaningful to make a quantitative comparison of

TABLE I. Energies, lifetimes, and the Franck–Condon (FC) factors of vibrational levels along the C–H stretching coordinate on the first electronically excited state $^3A''$ of the ethylene dication.

ν	Energy (eV)	Lifetime (ns)	FC factor
1	0.084	$>10^5$	1.25×10^{-1}
2	0.248	$>10^5$	2.17×10^{-1}
3	0.407	$>10^5$	2.17×10^{-1}
4	0.561	$>10^5$	1.63×10^{-1}
5	0.709	$>10^5$	1.04×10^{-1}
6	0.849	$>10^5$	5.91×10^{-2}
7	0.980	3.46×10^4	3.16×10^{-2}
8	1.099	2.53	1.63×10^{-2}
9	1.201	1.19×10^{-3}	8.15×10^{-3}

the computed lifetimes with the experimentally determined values. On the other hand, the lifetimes of the highest vibrational levels of the two excited states are on the order of femtoseconds and picoseconds, which is consistent with the prompt deprotonation process. Additionally, the prompt deprotonation could also originate from nuclear wave packets in the continuum populated above the dissociation barrier during double ionization.

From the calculated PECs we estimate KER values for fragmentations from the highest vibrational levels of the two electronically excited states to the dissociation limit. We obtain 3.7 and 3.5 eV for the delayed fragmentation from the first and the second electronic excited states, respectively, which is slightly smaller than the measured value of 4.1 eV.

A. Population mechanism of high-lying vibrational states

We now turn to the question how high-lying vibrational states can be populated during the interaction of a strong laser field with an ethylene molecule. Previous studies indicate that electronically excited states of ethylene dications can be populated directly through strong field double ionization by removing one or two electrons from lower-lying molecular orbitals [5,9,10].

TABLE II. Energies, lifetimes, and the FC factors of vibrational levels along the C–H stretching coordinate on the second electronically excited state $^1A''$ of the ethylene dication.

ν	Energy (eV)	Lifetime (ns)	FC factor
1	0.078	$>10^5$	7.70×10^{-2}
2	0.229	$>10^5$	1.61×10^{-1}
3	0.379	$>10^5$	1.92×10^{-1}
4	0.525	$>10^5$	1.71×10^{-1}
5	0.668	$>10^5$	1.27×10^{-1}
6	0.808	$>10^5$	8.27×10^{-2}
7	0.942	$>10^5$	4.94×10^{-2}
8	1.072	$>10^5$	2.77×10^{-2}
9	1.194	$>10^5$	1.50×10^{-2}
10	1.309	1.30×10^3	7.92×10^{-3}
11	1.413	3.00×10^{-1}	4.18×10^{-3}
12	1.501	3.86×10^{-4}	2.17×10^{-3}

In our measurements, the double ionization process happens within the very short duration of a few-cycle laser pulse. During this time the nuclei can be considered frozen in the neutral equilibrium geometry. From the simulations, listed in Tables I and II, we found that the Franck–Condon (FC) factors between the vibronic ground state of the neutral ethylene and vibrational excited states of the ethylene dication on the electronically excited states are on the order of 10^{-2} for the high-lying vibrational states that can dissociate through tunneling. This indicates that the high-lying vibrational states can be directly populated by strong field double ionization through removing at least one HOMO-1 electron. Note that the FC factors between the vibronic ground state of neutral ethylene and high-lying vibrational states on the electronic ground state of the ethylene dication are very small. Therefore the contribution from the electronic ground state to the slow deprotonation is unlikely.

B. Comparison between ethylene and acetylene

From acetylene measurements we retrieved the decay rate of long-lived acetylene dications in the same manner as for the measurements on ethylene. We found it as $(5.9 \pm 0.5) \times 10^{-4}$ ns^{-1} corresponding to a mean survival time of 1695 ± 144 ns, i.e., much longer than that of the ethylene dication. The relative channel strength of the delayed deprotonation to the prompt one for acetylene is 2.9%, which is almost the same as that of ethylene.

Although the signal corresponding to the slow deprotonation process is similar for ethylene and acetylene, the origin of this process is quite different for these two molecules. In the neutral state the main difference between the two species is that ethylene has a C–C double bond and acetylene has a C–C triple bond. Also their dications exhibit different electronic configurations.

As presented in Fig. 4(b), the three lowest electronic states ($^3\Sigma^-$, $^1\Delta$, and $^1\Sigma^+$) of the acetylene dication are metastable. The lowest state $^3\Sigma^-$ is the dicationic electronic ground state, which is a triplet state. It is formed by removal of two electrons with the same spin; one from the HOMO and the other one from the degenerate HOMO-1. The other two states ($^1\Delta$ and $^1\Sigma^+$) are, however, formed by removal of two electrons with different spins; either both from the HOMO or one from the HOMO and the other from HOMO-1. All three electronic states can be populated by strong-field induced double ionization. Similar to the electronic ground state of the ethylene dication, only low-lying vibrational levels will be dominantly populated during the double ionization process from the neutral acetylene due to rather small FC factors between high-lying vibrational states and the vibrational ground state of the neutral acetylene. The population in the low-lying vibrational states of the electronic ground state gives rise to the detected stable acetylene dications whose survival times are longer than their TOF to the detector. Similar to ethylene, to support the delayed deprotonation process, the nuclear wave packet needs to be prepared on a high-lying vibrational state near the dissociation threshold of an electronic state in the acetylene dication. Although direct population of near-threshold vibrational states during ionization is unlikely due to the small FC factors, the population in the two upper metastable electronic states can possibly decay nonradiatively into the high-lying vibrational states of the electronic ground state via a spin-flip transition (intersystem crossing). Some such populated high-lying vibrational states can be close to the dissociation threshold along the C–H stretching. From these states the nuclear wave packet might tunnel through the dissociation barrier and cause the observed delayed deprotonation.

Finally, we would like to note that an alternative explanation for the delayed deprotonation process of both ethylene and acetylene could be over-the-barrier dissociation. In this case the dissociation might, in principle, proceed from a metastable electronic state, on a vibrational state that has an energy slightly larger than the potential barrier. Although the one-dimensional model for the deprotonation along the C–H stretching coordinate suggests that the FC factors for the population of such above-barrier vibrational states should be very small for PECs similar to the neutral ground-state PEC (such as the electronic ground state of ethylene and the three lowest-lying electronic states of acetylene), it does not mean that the process is very unlikely. If one also considers the possibility of excitation to other vibrational modes, the such-created multidimensional vibrational wave packet could have larger energy than the barrier along the C–H stretching, while simultaneously its projection onto the C–H stretching coordinate could have a simple structure corresponding to a significant FC factor. This way, both above-barrier continuum states leading to prompt deprotonation, and above-barrier Feshbach-type resonances [40] leading to delayed deprotonation could be formed. Quantitative simulation of this mechanism, however, requires accurate global potential-energy surfaces and multidimensional wave-packet propagations, which is a formidable task, and was not attempted in this work. By using the Rice–Ramsperger–Kassel–Marcus (RRKM) theory, in Ref. [12], the rate constant k for the dissociation of $C_2H_2^{2+} \rightarrow C_2H^+ + H^+$ on the electronic ground triplet PES was estimated to be $k = 2.2 \times 10^{12}$ s^{-1} for a total internal energy of about 1 eV above the dissociation barrier. Although this value of k is too large to explain the experimentally measured μs-order lifetime, we note that k is expected to decrease if the total energy decreases to a value only slightly larger than the barrier height.

V. CONCLUSION

In conclusion, we experimentally and theoretically studied the delayed fragmentation of hydrocarbon dications following double ionization by a strong laser field. A possible scenario of the observed delayed deprotonation process in ethylene consistent with the simple theoretical model applied in this work is as follows: In the first step, an ethylene molecule is doubly ionized by removing at least one HOMO-1 electron. This prepares the dication in an electronically excited state. Following the Frank–Condon principle, high-lying vibrational states on the electronically excited states will be populated during strong field double ionization. These high-lying vibrational states can later tunnel through the dissociation barrier along the C–H stretch coordinate, which leads to the delayed deprotonation process. In acetylene, the delayed deprotonation process probably occurs from the near-dissociation-threshold

vibrational states on the dicationic electronic ground state. A possible mechanism for populating these vibrational states might be vibrational excitation via intersystem transitions from electronically excited states to the electronic ground state. Since vibrational excitation through double ionization and intersystem crossing are common processes in many molecular systems, the delayed deprotonation process observed in our experiments should play an important role in the strong-field interaction with a variety of polyatomic molecules. We think that the delayed fragmentation process described here could be harnessed for controlling chemical reactions taking place on nanosecond to microsecond timescales.

ACKNOWLEDGMENTS

We thank Dr. Artem Rudenko for helpful discussions. This work was financed by the Austrian Science Fund (FWF) under Grants No. P25615-N27, No. P28475-N27, No. P21463-N22, and No. P27491-N27 and No. SFB-F49 NEXTlite, by a starting grant from the ERC (project CyFi), by the Ministry of Education, Culture, Sports, Science and Technology (MEXT), Japan (Grant-in-Aid for Specially Promoted Research No. 19002006), and by the Grant-in-Aid (Tokubetsu Kenkyuin Shorei-hi) scientific research fund of JSPS (Japan Society for the Promotion of Science), and JSPS KAKENHI Grant No. 15H05696.

[1] A. H. Zewail, Science **242**, 1645 (1988).
[2] A. H. Zewail, J. Phys. Chem. A **104**, 5660 (2000).
[3] A. Assion, T. Baumert, M. Bergt, T. Brixner, B. Kiefer, V. Seyfried, M. Strehle, and G. Gerber, Science **282**, 919 (1998).
[4] Y. Liu, X. Liu, Y. Deng, C. Wu, H. Jiang, and Q. Gong, Phys. Rev. Lett. **106**, 073004 (2011).
[5] X. Xie, K. Doblhoff-Dier, S. Roither, M. S. Schöffler, D. Kartashov, H. Xu, T. Rathje, G. G. Paulus, A. Baltuška, S. Gräfe, and M. Kitzler, Phys. Rev. Lett. **109**, 243001 (2012).
[6] M. F. Kling, P. von den Hoff, I. Znakovskaya, and R. de Vivie-Riedle, Phys. Chem. Chem. Phys. **15**, 9448 (2013).
[7] E. Wells, C. E. Rallis, M. Zohrabi, R. Siemering, B. Jochim, P. R. Andrews, U. Ablikim, B. Gaire, S. De, K. D. Carnes *et al.*, Nat. Commun. **4**, 2895 (2013).
[8] A. S. Alnaser, M. Kübel, R. Siemering, B. Bergues, N. G. Kling, K. J. Betsch, Y. Deng, J. Schmidt, Z. A. Alahmed, A. M. Azzeer *et al.*, Nat. Commun. **5**, 3800 (2014).
[9] X. Xie, S. Roither, M. Schöffler, E. Lötstedt, D. Kartashov, L. Zhang, G. G. Paulus, A. Iwasaki, A. Baltuška, K. Yamanouchi, and M. Kitzler, Phys. Rev. X **4**, 021005 (2014).
[10] X. Xie, K. Doblhoff-Dier, H. Xu, S. Roither, M. S. Schöffler, D. Kartashov, S. Erattupuzha, T. Rathje, G. G. Paulus, K. Yamanouchi, A. Baltuška, S. Gräfe, and M. Kitzler, Phys. Rev. Lett. **112**, 163003 (2014).
[11] K. Yamanouchi, Science **295**, 1659 (2002).
[12] T. S. Zyubina, Y. A. Dyakov, S. H. Lin, A. D. Bandrauk, and A. M. Mebel, J. Chem. Phys. **123**, 134320 (2005).
[13] A. S. Alnaser, I. Litvinyuk, T. Osipov, B. Ulrich, A. Landers, E. Wells, C. M. Maharjan, P. Ranitovic, I. Bocharevа, D. Ray, and C. L. Cocke, J. Phys. B: At., Mol. Opt. Phys. **39**, S485 (2006).
[14] A. S. Sandhu, E. Gagnon, R. Santra, V. Sharma, W. Li, P. Ho, P. Ranitovic, C. L. Cocke, M. M. Murnane, and H. C. Kapteyn, Science **322**, 1081 (2008).
[15] T. Osipov, T. N. Rescigno, T. Weber, S. Miyabe, T. Jahnke, A. S. Alnaser, M. P. Hertlein, O. Jagutzki, L. P. H. Schmidt, M. Schöffler, L. Foucar, S. Schössler, T. Havermeier, M. Odenweller, S. Voss, B. Feinberg, A. L. Landers, M. H. Prior, R. Dörner, C. L. Cocke, and A. Belkacem, J. Phys. B: At., Mol. Opt. Phys. **41**, 091001 (2008).
[16] X. Zhou, P. Ranitovic, C. W. Hogle, J. H. D. Eland, H. C. Kapteyn, and M. M. Murnane, Nat. Phys. **8**, 232 (2012).
[17] A. Talebpour, A. D. Bandrauk, J. Yang, and S. L. Chin, Chem. Phys. Lett. **313**, 789 (1999).
[18] B. Gaire, S. Y. Lee, D. J. Haxton, P. M. Pelz, I. Bocharova, F. P. Sturm, N. Gehrken, M. Honig, M. Pitzer, D. Metz, H.-K. Kim, M. Schöffler, R. Dörner, H. Gassert, S. Zeller, J. Voigtsberger, W. Cao, M. Zohrabi, J. Williams, A. Gatton, D. Reedy, C. Nook, T. Müller, A. L. Landers, C. L. Cocke, I. Ben-Itzhak, T. Jahnke, A. Belkacem, and T. Weber, Phys. Rev. A **89**, 013403 (2014).
[19] R. Dörner, V. Mergel, O. Jagutzki, J. U. L. Spielberger, R. Moshammer, and H. Schmidt-Böcking, Phys. Rep. **330**, 95 (2000).
[20] J. Ullrich, R. Moshammer, A. Dorn, R. Dörner, L. P. H. Schmidt, and H. Schmidt-Böcking, Rep. Prog. Phys. **66**, 1463 (2003).
[21] M. Bixon and J. Jortner, J. Chem. Phys. **48**, 715 (1968).
[22] C. Smeenk, J. Z. Salvail, L. Arissian, P. B. Corkum, C. T. Hebeisen, and A. Staudte, Opt. Express **19**, 9336 (2011).
[23] A. M. Sayler, T. Rathje, W. Müller, C. Kürbis, K. Rühle, G. Stibenz, and G. G. Paulus, Opt. Express **19**, 4464 (2011).
[24] A. M. Sayler, T. Rathje, W. Müller, K. Rühle, R. Kienberger, and G. G. Paulus, Opt. Lett. **36**, 1 (2011).
[25] L. Zhang, S. Roither, X. Xie, D. Kartashov, M. Schöffler, H. Xu, A. Iwasaki, S. Gräfe, T. Okino, K. Yamanouchi, A. Baltuska, and M. Kitzler, J. Phys. B: At., Mol. Opt. Phys. **45**, 085603 (2012).
[26] X. Xie, S. Roither, D. Kartashov, E. Persson, D. G. Arbó, L. Zhang, S. Gräfe, M. S. Schöffler, J. Burgdörfer, A. Baltuška, and M. Kitzler, Phys. Rev. Lett. **108**, 193004 (2012).
[27] T. A. Field and J. H. Eland, Chem. Phys. Lett. **211**, 436 (1993).
[28] D. Holland, D. Shaw, I. Sumner, M. Bowler, R. Mackie, L. Shpinkova, L. Cooper, E. Rennie, J. Parker, and C. Johnson, Int. J. Mass Spectrom. **220**, 31 (2002).
[29] A. E. Slattery, T. A. Field, M. Ahmad, R. I. Hall, J. Lambourne, F. Penent, P. Lablanquie, and J. H. D. Eland, J. Chem. Phys. **122**, 084317 (2005).
[30] M. Alagia, P. Candori, S. Falcinelli, M. S. P. Mundim, F. Pirani, R. Richter, M. Rosi, S. Stranges, and F. Vecchiocattivi, J. Chem. Phys. **135**, 144304 (2011).
[31] M. Alagia, C. Callegari, P. Candori, S. Falcinelli, F. Pirani, R. Richter, S. Stranges, and F. Vecchiocattivi, J. Chem. Phys. **136**, 204302 (2012).
[32] M. Alagia, P. Candori, S. Falcinelli, K. Mundim, M. Mundim, F. Pirani, R. Richter, S. Stranges, and F. Vecchiocattivi, Chem. Phys. **398**, 134 (2012).
[33] V. Dribinski, A. Ossadtchi, V. A. Mandelshtam, and H. Reisler, Rev. Sci. Instrum. **73**, 2634 (2002).
[34] S. Roither, X. Xie, D. Kartashov, L. Zhang, M. Schöffler, H. Xu, A. Iwasaki, T. Okino, K. Yamanouchi, A. Baltuska, and M. Kitzler, Phys. Rev. Lett. **106**, 163001 (2011).

[35] X. Xie, S. Roither, M. Schöffler, H. Xu, S. Bubin, E. Lötstedt, S. Erattuphuza, A. Iwasaki, D. Kartashov, K. Varga, G. G. Paulus, A. Baltuška, K. Yamanouchi, and M. Kitzler, Phys. Rev. A **89**, 023429 (2014).

[36] X. Xie, E. Lötstedt, S. Roither, M. Schöffler, D. Kartashov, K. Midorikawa, A. Baltuška, K. Yamanouchi, and M. Kitzler, Sci. Rep. **5**, 12877 (2015).

[37] M. W. Schmidt, K. K. Baldridge, J. A. Boatz, S. T. Elbert, M. S. Gordon, J. H. Jensen, S. Koseki, N. Matsunaga, K. A. Nguyen, S. Su, T. L. Windus, M. Dupuis, and J. A. Montgomery, Jr., J. Comput. Chem. **14**, 1347 (1993).

[38] W. P. Reinhardt, Annu. Rev. Phys. Chem. **33**, 223 (1982).

[39] S. Klaiman and I. Gilary, Adv. At. Mol. Opt. Phys. **63**, 1 (2012).

[40] N. Moiseyev, Phys. Rep. **302**, 212 (1998).